Chapter 2

Nanotube cleaning, functionalization, characterization, metal removal and adsorption isotherm studies

Chapter - 2

Nanotube cleaning, functionalization, characterization, metal removal and Adsorption Isotherm studies

2.1 Introduction

There have been reports of existence of carbon nanotubes with nanometer diameters in seventies by scientists working on different forms of graphite, in France and Japan. In Russia, LV Radushkevich reported about carbon nanotubes in 1952. M Endo from Japan and A Oberlin from France first observed nanotubes in 1976. But these were brought into limelight by Iijima in 1991. Since then they have been the subject of increasing numbers of experimental and theoretical studies. Because of their unique mechanical, electrical, optical and thermal properties (as already discussed in previous chapter) CNTs can be used to prepare novel materials such as hydrogen storage materials, super conductors, reinforced materials etc. On the mass basis they have much larger surface area than bulk particles and can also be functionalized with various chemical groups to increase their affinity towards target species[114].

Having known about the hazardous and mutagenic effects of traces of heavy metal ions in water, and a thousand approaches to remove them, the CNTs capture the title of being one of the most effective sources, for the purpose. Adsorption technique is very popular due to simplicity and low cost. In an adsorption process, atom or ions (adsorbate) in a fluid phase diffuse to the surface of a solid (adsorbent), where they bond with the solid surface or are held there by weak intermolecular forces. Although activated carbon[115,116] is frequently used as general adsorbent of inorganic and organic compounds, alternative adsorbents have been developed. Many adsorbents have been developed and used to remove metal ions from waste water such as hybrid EDTA-zirconium phosphate cation exchanger [117], hazelnut activated carbon [118], peanut hulls [119]and chelating resin [120].The use of activated carbon, metal oxides and silica with various reagents utilized for removal has also been frequently practiced [121-123].CNTs, on account of large surface areas, very high adsorptive nature, hydrophobic inner walls and resistant to bacterial contamination have been introduced recently in water purification applications as an efficient adsorbent and reported for removal of different heavy metal ions like Pb(II), Cd(II), As(III) etc.[124,125]

However, there are many difficulties encountered in the synthesis of high quality nanotube samples and so their direct use can also be questioned. The various methods used for nanotube synthesis such as Arc discharge, Laser ablation, Chemical vapour deposition, High Pressure Carbon monoxide synthesis etc involve traces of heavy metals such as Fe, Co, Ni and many amorphous and carbonaceous forms of carbon. Furthermore, nanoparticles consisting of nested closed graphitic layers of polyhedral shape make up to one half in weight of the nanomaterial deposit. The nanotubes which are produced are of different dimensions. They are with a wide distribution of lengths, helicities of the layers, and diameters.

Up to now, the only available purification method was oxidation, either in gas-phase [126,127]or in liquid-phase[128,129]. The basal planes of graphite are subject to oxidation only if defects (vacancies/dislocations) are present. The tips of the tubes and the particles, incorporating reactive five-membered carbon rings, have a higher curvature and higher strain and will thus be preferentially attacked [131].The tube ends get invariably opened or at least damaged during the purification process, and the outer tube layers are removed during the treatment, presumably because of defects in the hexagonal network [130]. Tube tips have electronic properties that differ from the cylindrical part of the nanotubes [132], and they determine furthermore to a great extent the field emission properties and various other properties of the tubes. It is so of great importance to obtain purified tubes with intact ends and non-damaged sidewalls.

Cleaning of nanotubes would help to explore the properties better. Surface purification followed by functionalization with various groups could help to increase the activity of nanotubes. This work is focused on exploring the adsorption properties of surface and chelation properties of the functional groups decorating their surface. These properties have been studied in detail for heavy metal rejection from aqueous solutions. Studies have been done varying the metal ion concentration, CNT dosage, time of contact of the two and pH of prepared solution. Modifications with different functional groups containing different atoms still increases the metal binding capacity of CNT (due to increased chelation or complexation) and helps to retain more heavy metal ions on the surface, and thus better rejection.

2.2 Materials

Carbon nanotubes (multi-walled carbon nanotubes, MWNTs) manufactured by HiPCO (supplied by Iljin Nanotech, Korea) whose purity was greater than 90%, were purchased from Sigma Aldrich. The MWNTs were of diameter 110-170 nm and length 5-9 microns. Conc. H_2SO_4 (98%), conc. HNO_3 GR (69%) were purchased from MERCK. $SOCl_2$, Ethylenediamine (>99%, Sigma Aldrich), Sodium azide (>99%, Sigma Aldrich) were used as it is.

2.3 Experiments

2.3.1 Surface cleaning of nanotubes

Cleaning of surface of these pristine CNTs with SDS (sodium dodecyl sulfate) has been previously reported[133]. A modified method for effective cleaning of surface was adopted and this method helps to remove the amorphous carbon soot and nearly all heavy metals present in the as purchased CNTs. In this process, 2g of the as purchased pristine nanotubes (HiPCO, >90%) were sonicated with 500 ml of 1% Brij 98 (a non-ionic surfactant) for about 2h. The sonicated solution was allowed to stand for about 6h. The added surfactant being greater than the CMC value, was able to make big micelle structures and remove the heavy soot by sedimentation (gravitational law). The sediment was rejected as soot associated with the nanotubes. The nanotubes were collected from the mother liquor by subsequent centrifugation and sedimentation at 3000 rpm for 15 minutes. This process was repeated 2-3 times to obtain nanotubes.

The surfactant associated with the nanotubes could be easily removed by alternate washing with water and brine solution. Some of the heavy metals that may have remain attached to the surface of the CNT's, were removed by converting these heavy metals into their soluble salts using 50% HCl solution. This separated the nanotubes from heavy metal chlorides thus giving a clean surface of the nanotubes. The yield was nearly 35% of the initial raw CNTs (2 g) used. The remaining 65% could be considered to be amorphous, other undesired carbonaceous material and heavy metal traces.

The obtained nanotubes do not get attracted to the magnetic needle showing that the nanotubes are free from traces of heavy metal ions. It differs from the pristine CNTs which contain Fe, Co, Ni and other trace metals, and get stuck to the magnetic needle. The SEM photograph of pristine nanotubes (Figure 2.1) clearly shows presence of amorphous and carbonaceous materials associated with nanotubes where pristine stock dominates and nanotubes are not visible. Purification and washing removes the unwanted carbonaceous material and metal ions and nanotube surfaces become clearly visible. Now these washed and dried nanotubes were used to treat with various functionalizing agents.

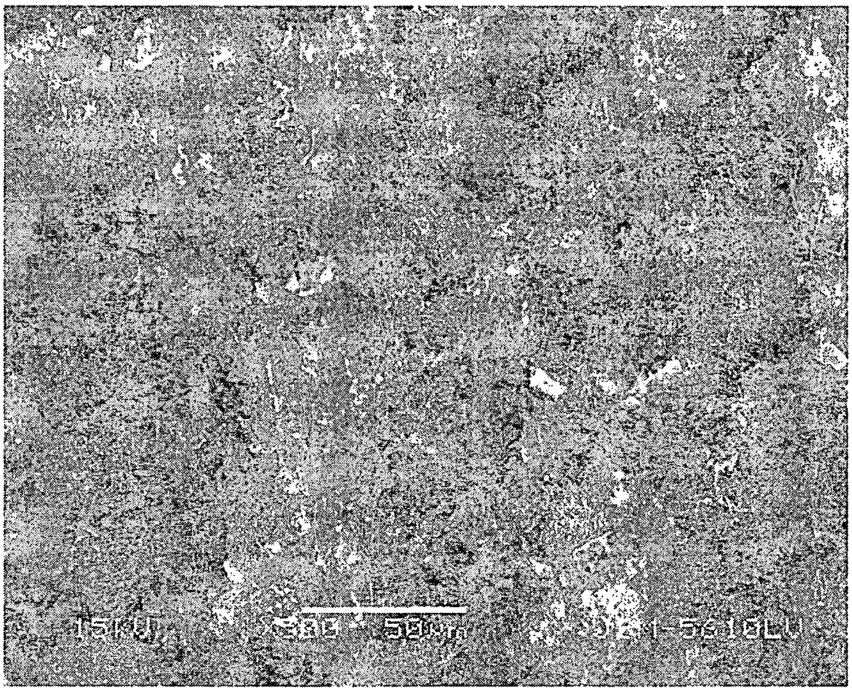

Figure 2.1 SEM image of commercially available Pristine CNTs.

2.3.2 Functionalization of CNTs

2.3.2.1 Oxidation of Carbon Nanotubes: The as-received and purified HiPCO MWNTs were first treated with a 3:1 mixture of concentrated nitric and sulfuric acid (40 mL). This acidic mixture is highly corrosive and reactive. This mixture was then stirred for 24 h at 40°C to introduce carboxylic acid groups on the MWCNT surface. The oxidized nanotubes were washed with double distilled water five times, to obtain oxidized clean surfaces of MWNT's.

Carboxylation is the most favored starting point because it can be covalently bonded to form ester or amide linkages easily .The sample was then dried in a vacuum oven at 80 °C for 4 h.

2.3.2.2 Acylation of Carbon Nanotubes: The oxidized nanotubes were treated with $SOCl_2$ to introduce the acyl groups. 200 mg of obtained nanotubes were added to 20 mL of thionyl chloride and 2mL of DMF (dimethyl formamide) in 100 mL round bottom flask. The system was properly sealed with grease and teflon, to prevent any moisture contamination and then refluxed for 36 hrs. at 60°C.The whole set up was put in hood and the excess of thionyl chloride was removed by boiling it off in hood.

The product obtained was washed with toluene .The sample was then dried in a vacuum oven at 80 °C for 4 h.

2.3.2.3 Functionalization of Carbon Nanotubes with Ethylenediamine:

Twenty milligrams of the acylated nanotubes (which contain –COCl distributed at places on the nanotube surface) were dispersed by sonication in 10 mL of ethylenediamine. The sonication was followed by stirring for 16 hrs. All processes were carried out at 60°C. The product was then diluted with 200 mL of methanol. The functionalized MWNTs were then dried in a vacuum oven at 80 °C for 4 h. This helped to introduce the amide groups on the CNT's.

2.3.2.4 Azide functionalization of carbon nanotubes:

Sodium Azide was used as a reagent to convert the –COCl group to –CON_3. 60 mg of acylated nanotubes were treated with 5 mg of NaN_3 in DMF as solvent (Figure 2.2). The azide linkageis highly reactive and thus reactions were done in controlled conditions and in absence of water. The reaction was carried out at 60°Cfor 16h, and finally the product is precipitated in toluene. The product was dried in oven at 80°C for 4 h.

2.3.3 Preparation of stocks and Batch method studies

Aqueous solutions of salts of Cr^{+6}, Pb^{+2}, Cd^{+2}, As^{+3}, $Cu^{+2}$and Ni^{+2}were prepared to study the absorptive strength of nanotubes. Stock solutions of chromium and lead of 1000 mg/l concentration were prepared by dissolving, 2.848 g of $K_2Cr_2O_7$, 1.598 g of $Pb(NO_3)_2$, respectively in 1000 ml of ultrapure water (Elix, Millipore), whereas cadmium solution was prepared by dissolving 1 g ofcadmium metal in minimum volume of (1 + 1) HCl and then making it up to 1000 ml with ultrapure water. Stock solution of nickel was prepared by dissolving 1.273 g of NiO in minimum volume of 10% (v/v) HCl and then diluted up to 1000 ml with ultrapure water. Standard working solutions of copper and arsenic were prepared from 1000 mg/L standard solution (Merck, Germany) and solutions of varying initial concentrations were prepared from a 1000 mg/L by serial dilution using distilled deionized water. In another series of experiments, the pH of Chromium metal ion solution was adjusted to 3.5 and 7.2 by the addition of 0.1N solution of NaOH during dilution process. Adsorption studies for other metal ions were done only at pH 3.5, as at basic pH they showed hydrolysis and hydroxides formation.

Batch experiments were carried out in different stoppered glass bottles at room temperature (25±1 ◦C) using known amount, i.e. 10mg of differently functionalized CNTs in 10 ml of metal ion concentration (1000μg/L) solution in ordinary mixing conditions using rotary shaker (Revotech) at the stirring speed of 120 rpm.

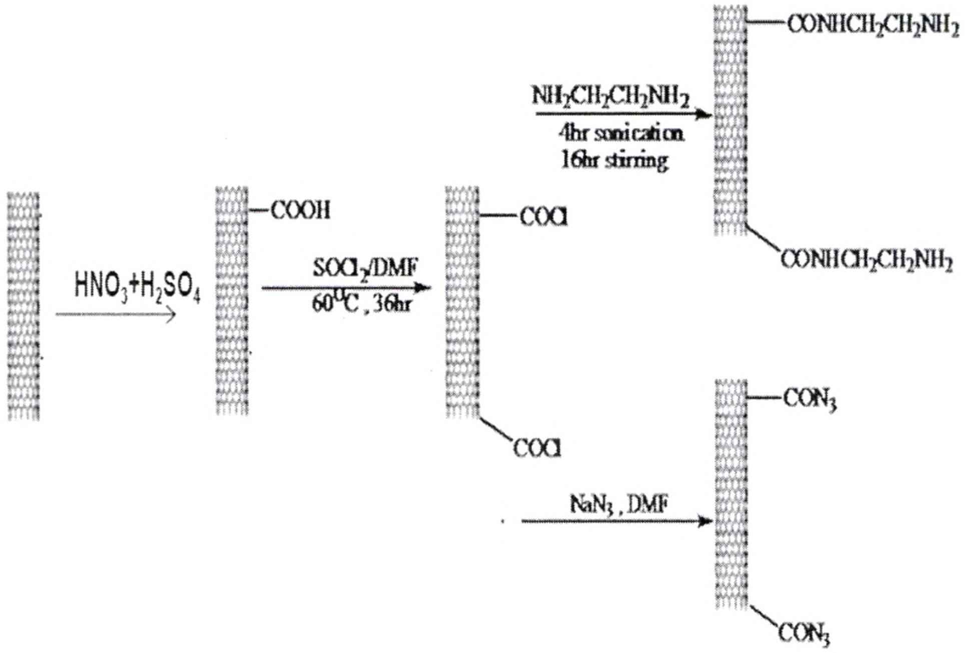

Figure 2.2 Schematic representation of functionalization of nanotubes.

The samples were taken after regular time interval and filtered through Whatman's filter paper. Concentrations of metal ions in filtrates were determined by AAS. These data were used for comparative removal studies and kinetic establishment. The Arsenic ion concentration was measured in graphite furnace mode of AAS and other metal were measured in flame mode of AAS. Blank experiments (without CNT) were conducted to confirm, no adsorption onto container walls.

2.4 *Characterization*

Concentrations of metal ions in filtrates were determined using Atomic Absorption Spectrophotometer (Analytikjena model Nova 400). AAS equipped with 100 mm burner, a cross flow nebulizer 5.0 ml/min and 1.2 mm slit was used throughout the experiments.IR spectra were recorded on Jasco FT-IR spectrometer model 610 by using KBr pellets. The pH measurements were made on a digital pH meter (HACH, sension 1, model 51935-00) equipped with a gel-filled pH electrode. The meter was calibrated with the buffers of 3.5 and 7.2.Raman spectra were recorded using microscope equipped triple monochromator combined with a peltier cooled charge couple device detector system. The spectra were acquired in the back-scattering geometry, while for excitation the 785 nm line of an Ar+ laser was focused on the sample by means of an 80· objective at a power of _2mW,measured directly before the sample. The phonon frequencies were obtained by fitting Lorentzian line shapes to the experimental peaks after background subtraction.

2.5 *Results and discussion*

2.5.1 Characterization of nanotubes

2.5.1.1 Raman spectroscopy

It is a reliable technique for the characterization of carbon-based nanostructures. It points at the various radial breathing and tangential stretching modes of vibrations. The vibrations corresponding to radial breathing mode at 785nm laser wavelength are very weak and not significant. The Raman spectra of MWNTs excited with this laser line show two characteristic bands in tangential stretching mode, namely the D-band at 1340-1390 cm^{-1}, and a G-band in the range1550-1600 cm^{-1}. The D-band is a disorder induced feature arising from double resonance scattering process and its intensity is a measure of defect concentration on the nanotubes. This defect is supposed to be created due various purification reactions, to which the nanotubes are exposed or heteroatom associated at time of growth of nanotubes or disordered carbon. The G band originates from in-plane tangential stretching of the carbon- carbon bonds in graphene sheets.

The D-band in graphite involves scattering from defect which breaks the basic symmetry [134,135] of the graphene sheet. It is observed in sp^2 carbons containing porous, impurities or other symmetry-breaking defects. Multi-walled carbon nanotubes (MWNT) are made of concentric graphene sheets rolled in a cylindrical form with diameters of tens of nanometers [136]and because of this large diameter of the outer tubes for typical MWNT and because they contain an ensemble of carbon nanotubes with diameters ranging from small to very large, most of the characteristic differences that distinguish the Raman spectra in SWNT from the spectra for graphite are not so evident in MWNT.

The Raman spectra as shown in (Figure 2.3) for pristine and purified CNT's bring out the fact that the I_D/I_G ratio (Intensity of D band / Intensity of G band) for pristine MWNT's is very high (intensity of D-band being more). This is in accordance with presence of amorphous and carbonaceous impurities, associated with as prepared CNT's, making the surface rough due to defects and disorders. Effective cleaning of the surfaces removes the unwanted materials and thus reducing the intensity of D-band. The I_D/I_G ratio of pristine nanotubes is 0.6665 which is reduced to 0.2366 in purified nanotubes, thus confirming effecting cleaning.

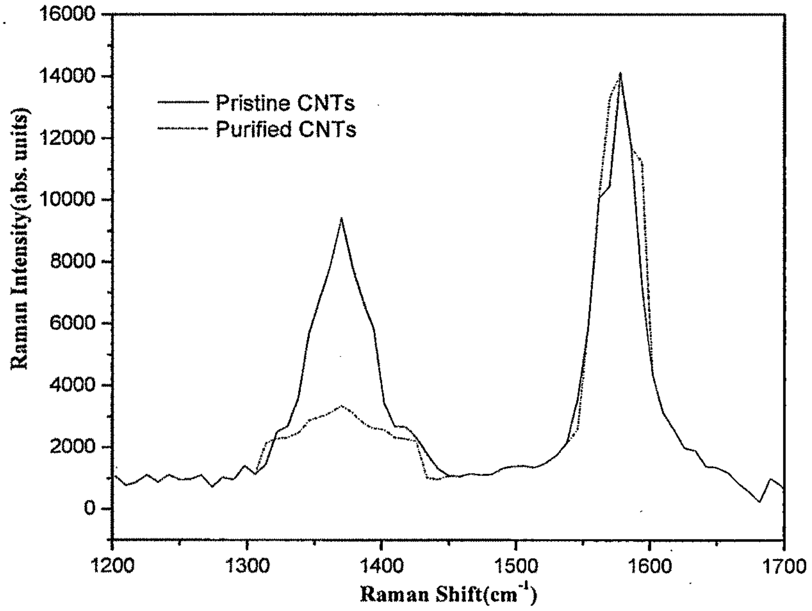

Figure 2.3 Raman spectra (a) Pristine (b) Purified CNTs.

2.5.1.2 Transmission Electron Microscopy

Nanotubes structures with cleaned surfaces and ends are visible in TEM images (Figure 2.4) of functionalized MWNTs. Pristine tubes have amorphous materials associated with them which is removed after cleaning and functionalization. The process ruptures the surface but, this damage is limited to the surface of the nanotube and the internal tubes remain intact. TEM images of cleaned and differently functionalized nanotubes reveal the open tips or ends, and different surface morphologies depending the functionalizing reagent and its strength. Nanotubes appear to have bamboo like structure. There is an outer graphitized layer and the inner tube is subdivided by single or multigraphite layers, which may be caused by surface diffusion of carbon cluster on large catalytic particle across nanotube wall (Li. D.C.; Dai. L. *Chem. Phys. Lett.* **2000**, *316*, 349).The commercially available nanotubes had an average 5-9μ length, which is reduced to 4-6 μ for some nanotubes as a result of functionalization.

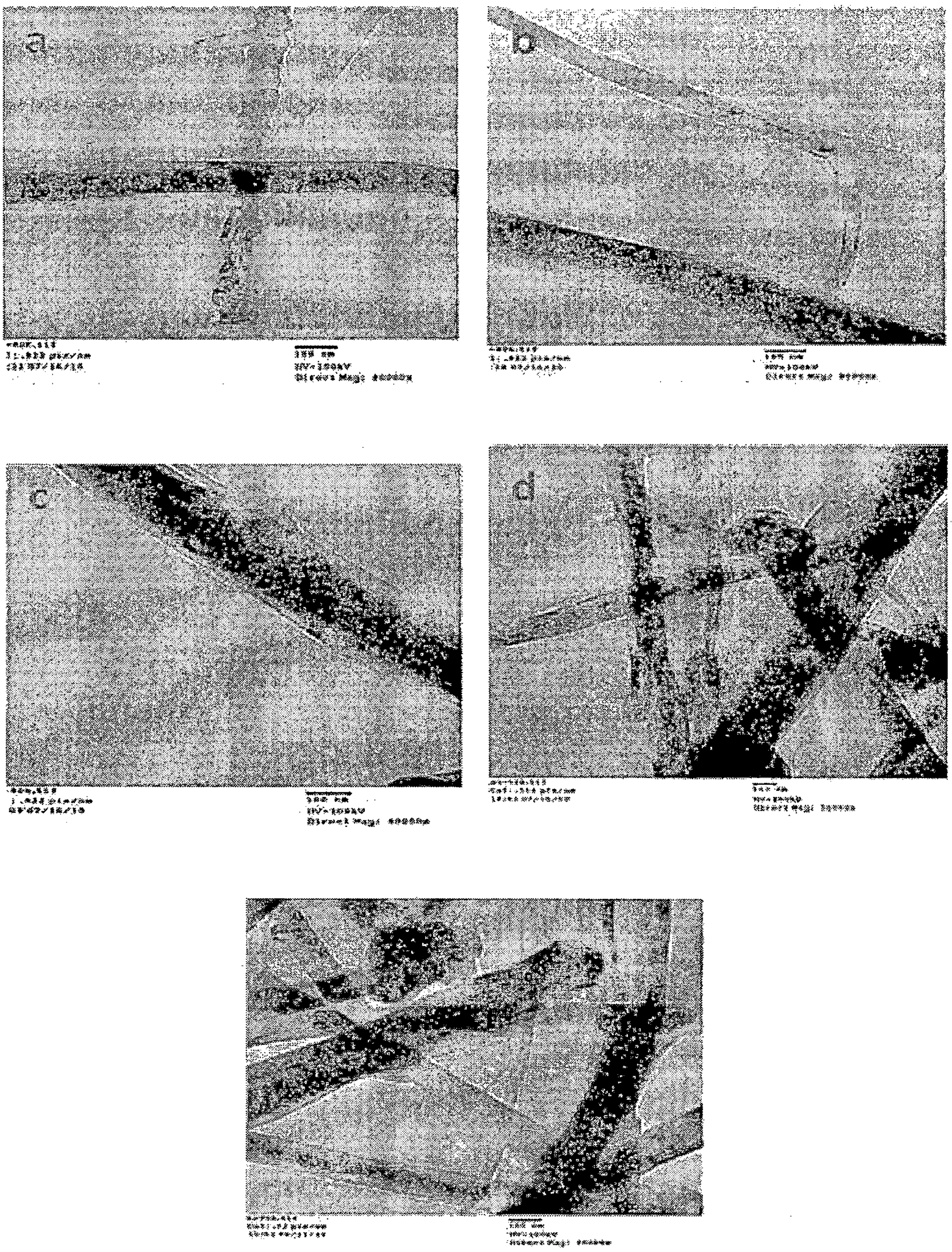

Figure 2.4 TEM images (a) Pristine (b) Oxidized (c) Acylated (d) Amide (e) Azide functionalized CNTs.

2.5.1.3 The FT-IR spectroscopy

The FT-IR spectra (Figure 2.5) of purified MWNTs (a) do not show any significant peaks, whereas the spectra of oxidized MWNT's (b) show a sharp band at 3500cm^{-1} due to hydroxyl(-OH) group. Band at 1726cm^{-1} could be due to the presence of C=O stretching of carboxylic group. Similarly the strong peak at 1618cm^{-1} can be assigned to C-O stretching of carboxylic group. Presence of carboxylate anion can also be confirmed by bands present in the range of 1460cm^{-1}. FTIR spectra of amide functionalized CNT's showed disappearance of the band at 1726 cm^{-1} and appearance of a new band at lower wave number (1633.41 cm^{-1}) due to amide carbonyl stretch. In addition, presence of new band at 1391 cm^{-1}, corresponds to C-N bond stretching . In case of azide functionalized nanotubes, the bands at 2142 cm^{-1} and 1566 cm^{-1} corresponds to asymmetric stretching and a weak symmetric stretching of azide functional group, for azide functionalized CNTs. The process thus helped to create sufficient functional groups on nanotubes surfaces (confirmed by titration).

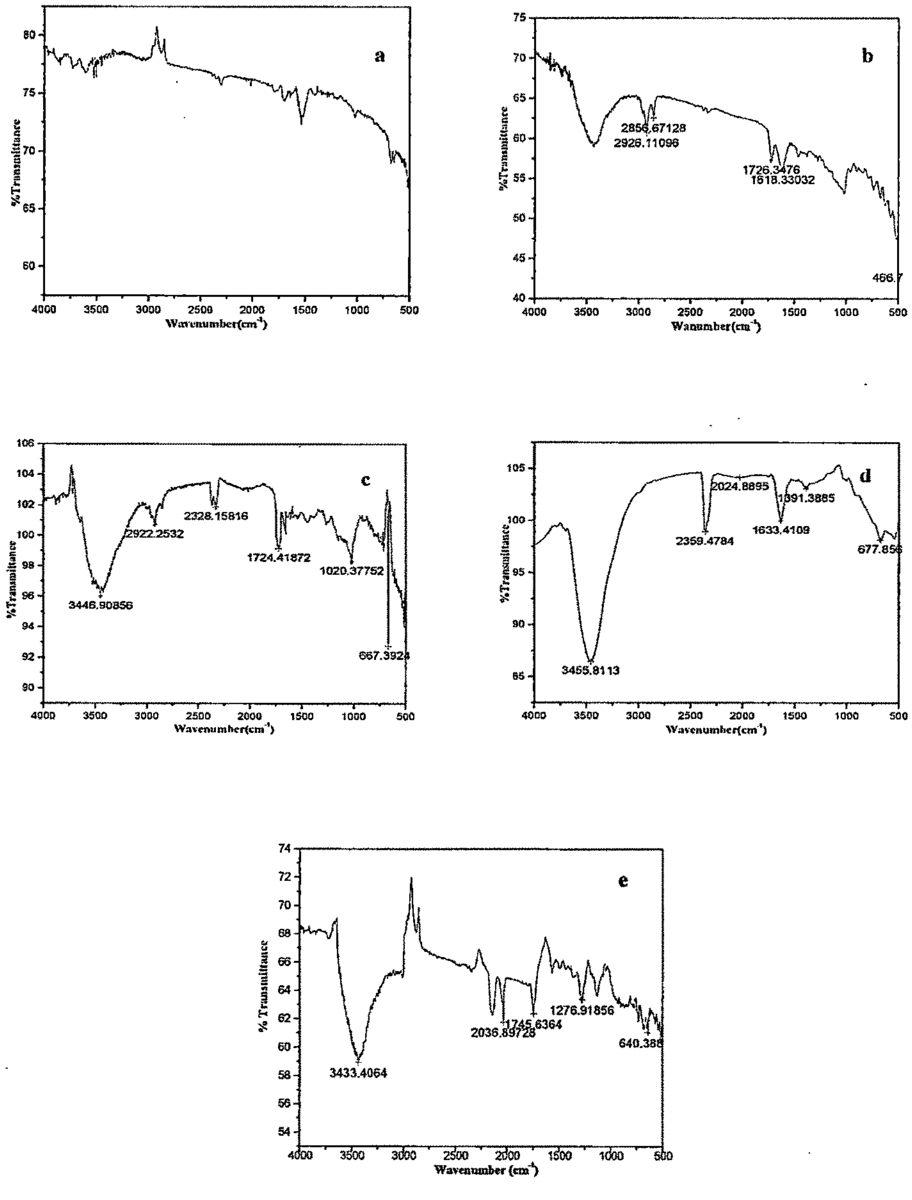

Figure 2.5 FT-IR spectras (a) Pristine (b) Oxidized (c) Acylated (d) Amide (e) Azide functionalized CNTs.

2.5.1.4 EDS spectral studies

The EDS spectral studies (Figure 2.6) of CNTs completely reveal the presence of different elements on their surfaces. EDS spectra of pristine CNT (Figure 2.6a) does not show any elemental peak except that of carbon, but elemental peaks of oxygen (Figure 2.6b) and nitrogen (Figure 2.6c) are clearly visible in oxidized and azide functionalized CNTs respectively, which confirm that CNTs have been functionalized by oxygen containing and nitrogen containing groups respectively.

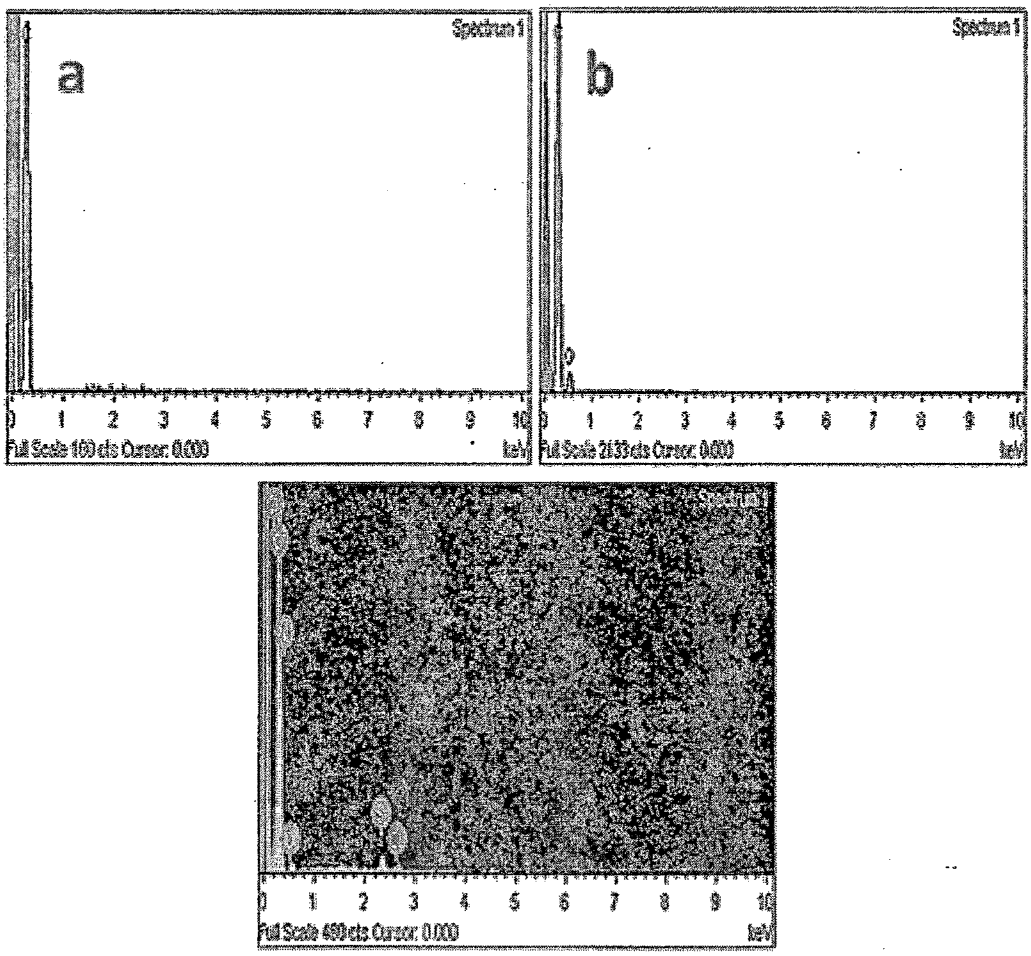

Figure 2.6 EDS spectras (a) Pristine (b) Oxidized (c) Azide functionalized CNTs.

2.5.1.5 X-Ray Diffraction studies

Since CNTs are having basic graphitized carbon with sp^2 hybridization, the modification during functionalization may be easily find out by XRD analysis. Figure 2.7 represents comparative XRD patterns for oxidized and amide functionalized CNTs. It is observed clearly that a well crystalline graphitized structure with 002, 100 and 004 planes is present in both materials. This indicates that the crystalline nature of CNT remained unaffected during different steps of functionalization process and proves the presence of CNTs in their actual form after functionalization.

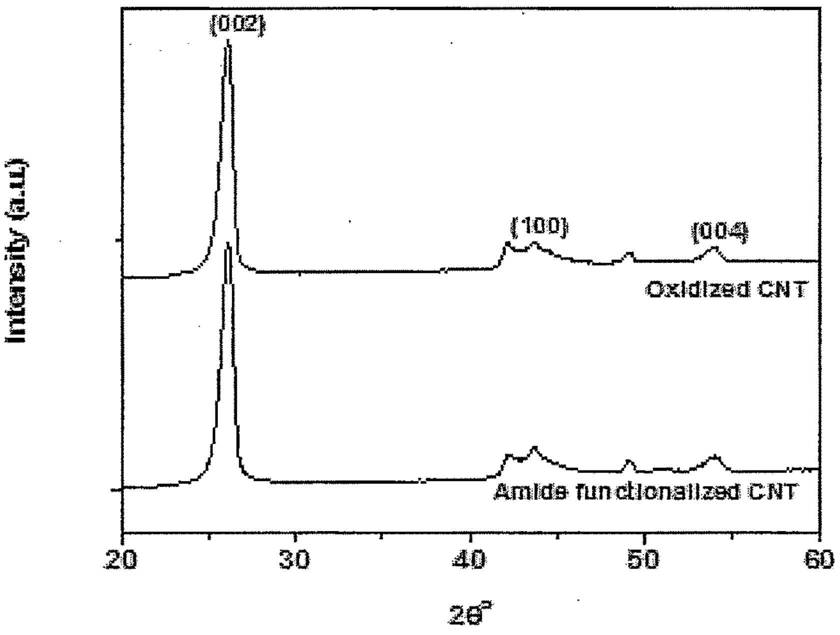

Figure 2.7 XRD spectra of oxidized and functionalized CNTs.

2.5.1.6 Thermo-gravimetric studies

Thermogravimetric studies reveal that functionalization of nanotubes disturbs the regular arrangement and geometry of hexagonal and pentagonal rings on the nanotube surface. The requirement of treatment with various reagents breaks the nanotube surface at various sites and thus reducing the thermal stability of nanotube structure. For purified nanotubes the disintegration occurs above 650°C, while disintegration temperature it is much lower for other functionalized CNT's (Figure 2.8).

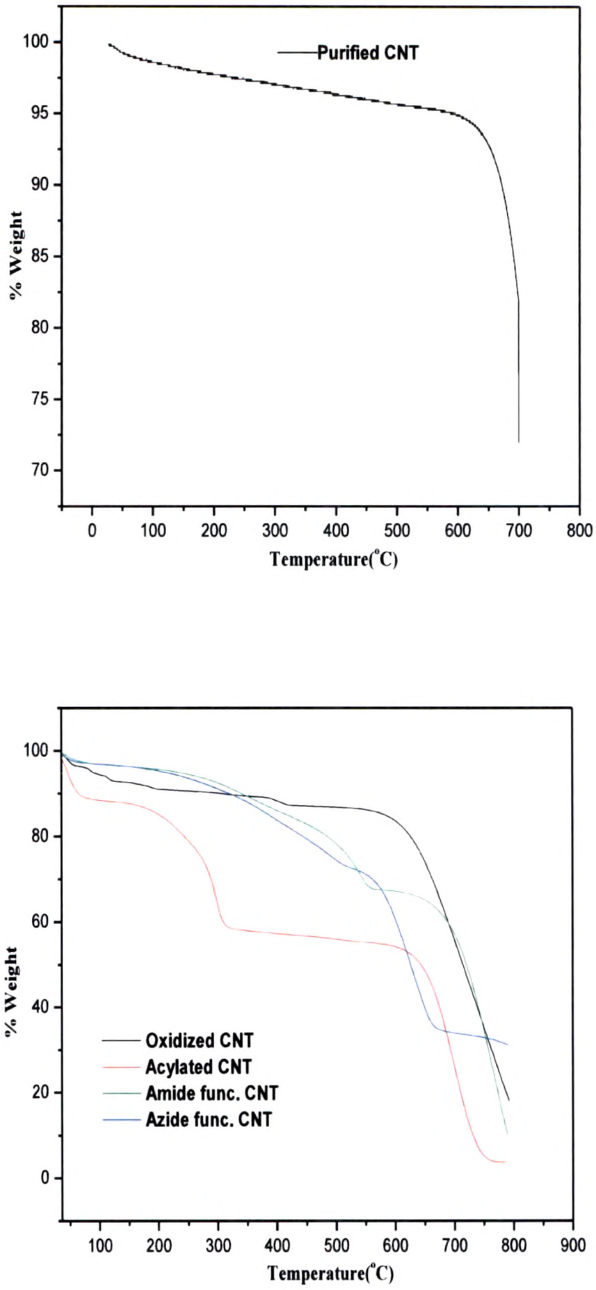

Figure 2.8 Thermo-gravimetric studies of Purified CNT's and various functionalized CNT's.

2.5.2 Adsorption kinetics

Heavy metal rejection studies were carried out for different metal ions. 1ppm solutions of Cr^{+6}, Pb^{+2}, Cu^{+2}, Cd^{+2}, As^{+3} and Ni^{+2}were prepared and batch experiments were carried out by putting 10mg each of differently functionalized CNT (oxidized, acylated, amide and azide functionalities) in 10 ml of metal ion solution in ordinary mixing conditions and stirred at speed of 120 rpm. The samples were taken after every 0.5h and filtered through Whatman's filter paper. Concentrations of metal ions in filtrates were determined by AAS.

2.5.2.1 Effect of time

Maximum adsorption and thus percentage removal is observed for Chromium (Figure 2.9a,2.10a,2.11a&2.12a, Table 2.1-2.4) followed by that of Lead, for all types of functionalized CNTs. The percentage uptake of all metal ion increases with increase in contact time. Increase in adsorption with time is greater for initial two hours, but then increase reduces and finally reaches a plateau. This point is equilibrium point where rate of adsorption is equal to rate of desorption from the surface. In all the cases equilibrium is reached at 3.5h where after no increase in uptake occurs with time of contact. At equilibrium the adsorption process becomes steady and does not increase with increase in contact period. The percentage rejections due to adsorption at surface of functionalized nanotubes were found to be much greater as compared to that by unfunctionalized stuff. Furthermore azide and amide functionalized CNTs proved more effective than the oxidized nanotubes (Table 2.5). This is explained by greater complexation tendency of azide and amide group with metal ion due to presence of hetero atoms nitrogen along with oxygen. The retained metal ions in form of complexes are also supported by adsorptive properties of CNTs, as the metal ions are retained on the surface due to two factors (a) chelate complex formation (b) strong adsorptive forces between metal ions and CNT surface, and the obtained water as filtrate from Whatman's filter paper is 40-90% free of hazardous heavy metal ions.

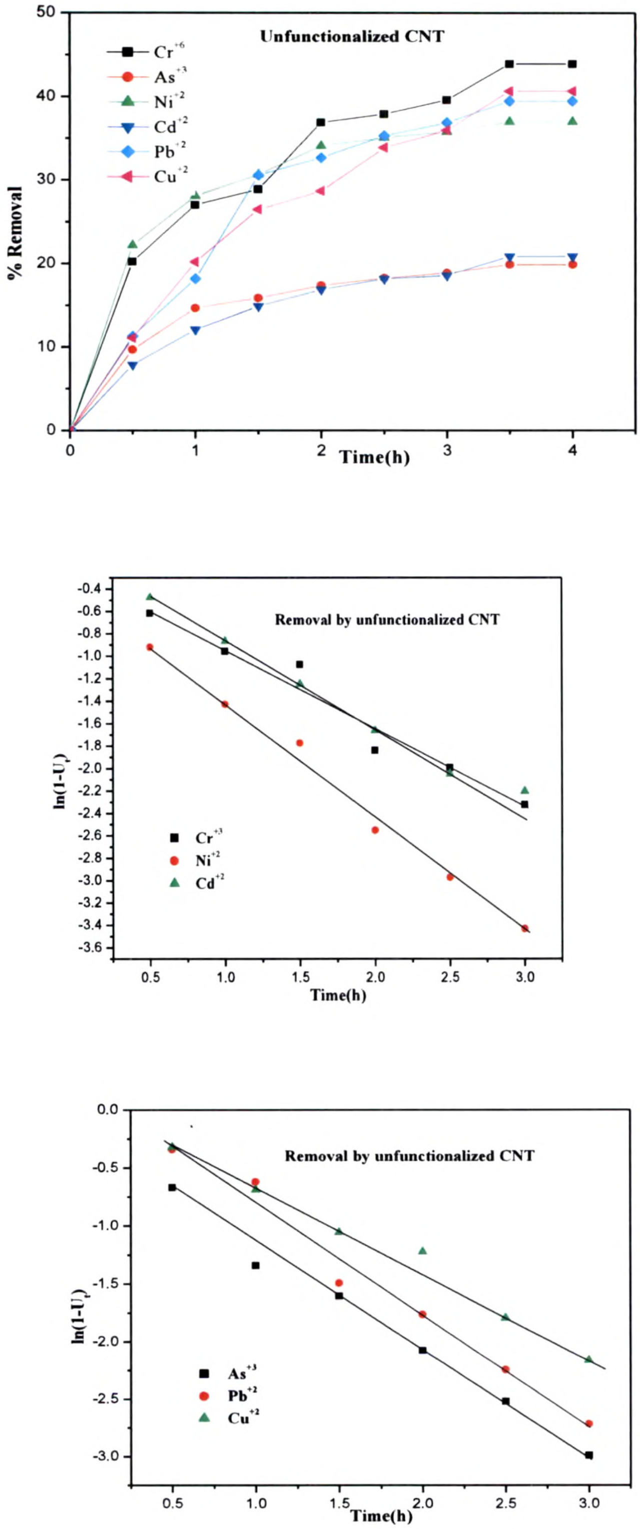

Figure 2.9 Plots of (a) % Removal of metal ions v/s time (b,c) $\ln(1\text{-}U_t)$ v/s Time(h) for removal of heavy metals by unfunctionalized CNTs.

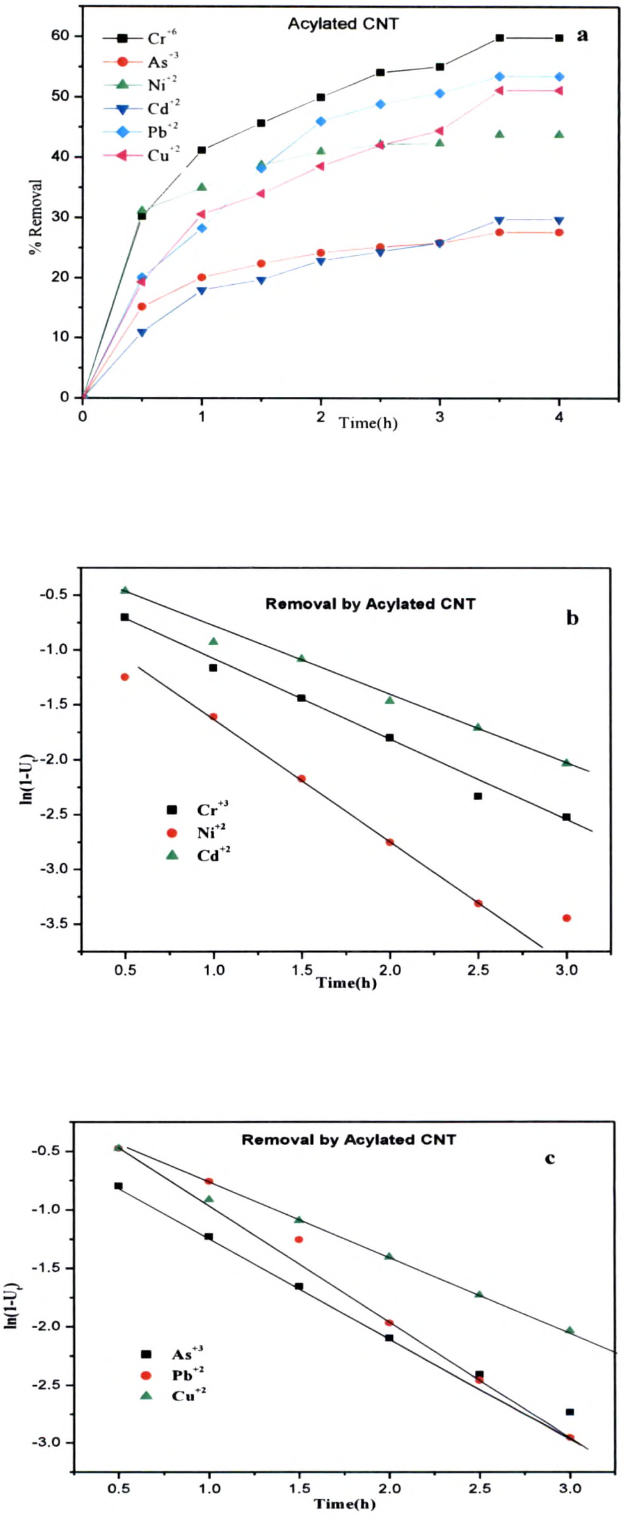

Figure 2.10 Plots of (a) % Removal of metal ions v/s time (b,c) ln(1-U_t) v/s Time(h) for removal of heavy metals by acylated CNTs.

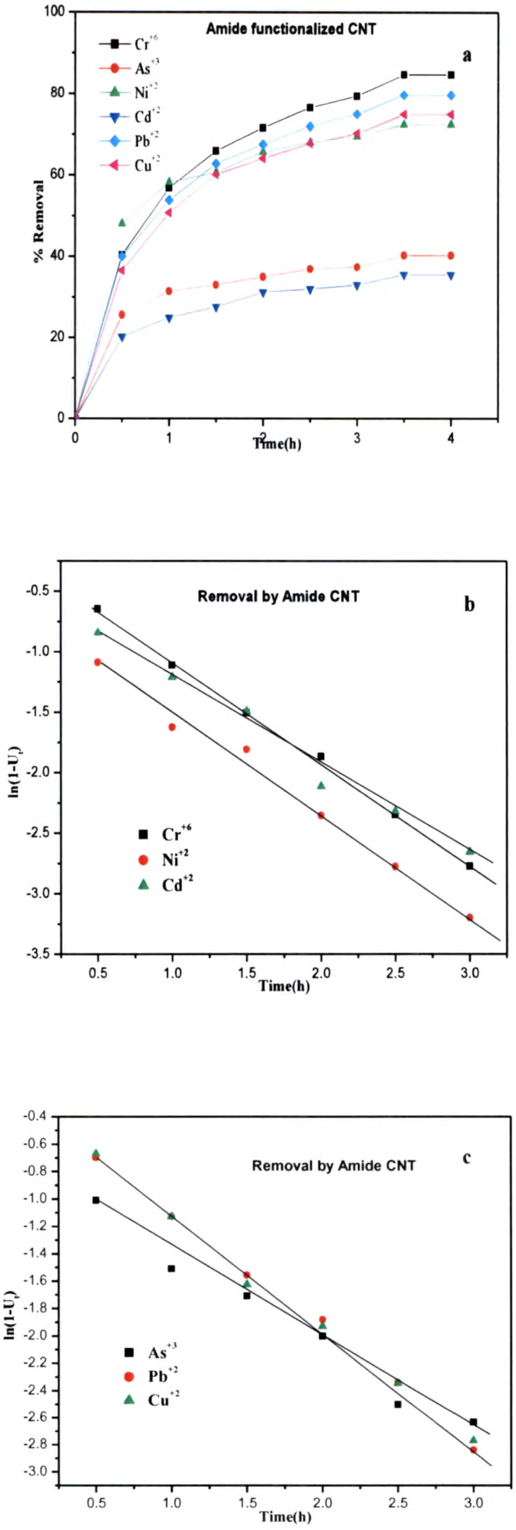

Figure 2.11 Plots of (a) % Removal of metal ions v/s time (b,c) $\ln(1-U_t)$ v/s Time(h) for removal of heavy metals by amide functionalized CNTs.

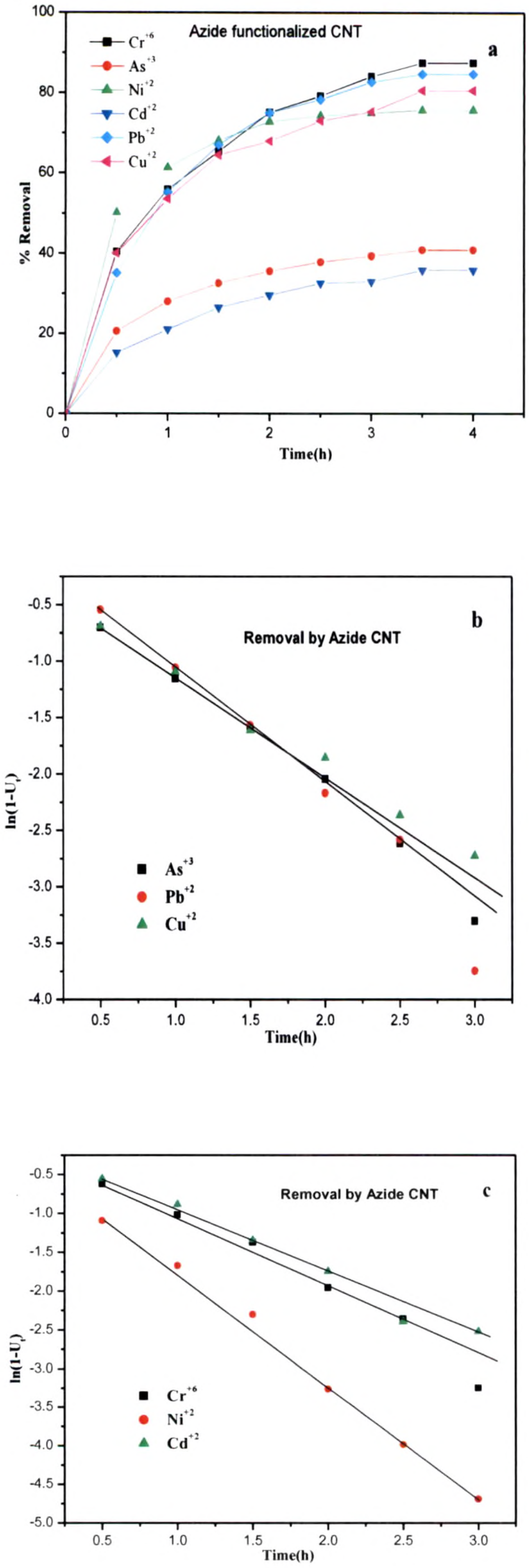

Figure 2.12 Plots of (a) % Removal of metal ions v/s time (b,c) ln(1-U_t) v/s Time(h) for removal of heavy metals by azide functionalized CNTs.

Table 2.1 % Removal of metal ions with time for unfunctionalized nanotubes.

S.No.	**Time (Hrs.)**	**Removal capacity (%) by unfunctionalized CNT**					
		Cr (VI)	**As (III)**	**Ni (II)**	**Cd (II)**	**Pb (II)**	**Cu (II)**
1	0.5	20.2	9.7	22.2	7.9	11.3	11.1
2	1.0	27.0	14.7	28.1	12.1	18.2	20.2
3	1.5	28.9	15.9	30.7	14.9	30.6	26.5
4	2.0	36.9	17.4	34.1	16.9	32.7	28.7
5	2.5	37.9	18.3	35.1	18.2	35.3	33.9
6	3.0	39.6	18.9	35.8	18.6	36.9	36.0
7	3.5	43.9	19.9	37.0	20.9	39.5	40.7
8	4.0	43.9	19.9	37.0	20.9	39.5	40.7

Table 2.2 % Removal of metal ions with time for acylated nanotubes.

S.No.	**Time (Hrs.)**	**Removal capacity (%) for acylated CNT's**					
		Cr (VI)	**As (III)**	**Ni (II)**	**Cd (II)**	**Pb (II)**	**Cu (II)**
1	0.5	30.2	15.2	31.2	11.0	20.1	19.3
2	1.0	41.2	20.1	35.0	18.0	28.3	30.6
3	1.5	45.7	22.4	38.8	19.7	38.2	34.0
4	2.0	50.0	24.2	41.0	22.9	46.0	38.6
5	2.5	54.1	25.2	42.2	24.4	48.9	42.1
6	3.0	55.1	25.9	42.4	25.9	50.7	44.5
7	3.5	59.9	27.7	43.8	29.8	53.5	51.2
8	4.0	59.9	27.7	43.8	29.8	53.5	51.2

Table 2.3 %Removal of metal ions with time for amide functionalized nanotubes.

S.No.	Time (Hrs.)	Removal capacity (%) for amide functionalized CNT's					
		Cr (VI)	**As (III)**	**Ni (II)**	**Cd (II)**	**Pb (II)**	**Cu (II)**
1	0.5	40.3	25.6	48.0	20.2	40.0	36.5
2	1.0	56.8	31.4	58.2	24.9	53.8	50.7
3	1.5	65.9	33.0	60.6	27.6	62.8	60.2
4	2.0	71.6	35.0	65.7	31.2	67.5	64.1
5	2.5	76.6	36.9	68.0	32.0	72.0	67.8
6	3.0	79.4	37.4	69.5	33.0	75.0	70.3
7	3.5	84.7	40.3	72.5	35.5	79.7	75.0
8	4.0	84.7	40.3	72.5	35.5	79.7	75.0

Table 2.4 %Removal of metal ions with time for azide functionalized nanotubes.

S.No.	Time (Hrs.)	Removal capacity (%) for azide functionalized CNT's					
		Cr (VI)	As (III)	Ni (II)	Cd (II)	Pb (II)	Cu (II)
1	0.5	40.4	20.6	50.2	15.2	35.1	40.1
2	1.0	55.9	28.0	61.4	21.0	55.2	53.6
3	1.5	65.3	32.6	68.1	26.5	67.0	64.5
4	2.0	75.1	35.6	72.8	29.6	75.0	68.0
5	2.5	79.2	37.9	74.3	32.6	78.3	73.0
6	3.0	84.1	39.4	75	33.0	82.7	75.3
7	3.5	87.5	40.9	75.7	35.9	84.7	80.6
8	4.0	87.5	40.9	75.7	35.9	84.7	80.6

Table 2.5 Comparative study of different MWNTs.

S.No.	**Time (Hrs.)**	**Removal capacity (%)**					
		Cr (VI)	**As (III)**	**Ni (II)**	**Cd (II)**	**Pb (II)**	**Cu (II)**
Without func. CNT	3.5	43.9	19.9	37.0	20.9	39.5	40.7
Oxidized CNT		59.6	25.2	41.9	27.3	52.5	45.8
Acylated CNT		59.9	27.7	43.8	29.8	53.5	51.2
Amide func. CNT		84.7	40.3	72.5	35.5	79.7	75.0
Azide func. CNT		87.5	40.9	75.7	35.9	84.7	80.6

Sorption process is greatly dependent on time of contact, pH and metal ion concentration, whose adsorption on an adsorbent has to be studied. Effect of pH and metal ion concentration, will be shortly studied later in this section. Adsorption of ions in an aqueous system follows reversible first order kinetics, when a single species is considered on a heterogeneous surface. The sorption of metal ion from solution phase onto adsorbent surface is a reversible reaction with forward rate constant k_1, backward rate constant k_2 and overall rate constant k ($k = k_1 + k_2$).

Taking 'a' as the initial concentration of metal ion and x is the amount adsorbed at time t, the reaction rate will be:

$$dx/dt) = -d(a-x)/dt = k(a-x) = k_1(a-x) - k_2x \quad (1)$$

Putting the value Xe as the concentration of metal adsorbed at equilibrium and Kc as the equilibrium constant, the equation at equilibrium($dx/dt = 0$):

$$Kc = X_e/a-X_e = k_1/k_2 \qquad (2)$$

Solving the above equation and using$U_t = x/X_e$, (U_t=fractional attainment of equilibrium) we get :

$$\ln (1-U_t) = -(k_1+k_2)t = -kt \qquad (3)$$

.Equation 3 states that, if a graph plotted between ln ($1-U_t$) and Time t gives a straight line with slope k, then the system follows first order kinetics.

The graphs plotted between ln ($1-U_t$) and Time t gave straight lines with negative slopes for all sets (Figure 2.9(b&c)-2.12(b&c)) from Tables 2.6-2.9, thus confirming the adsorption process to follow first order kinetics, for all functionalized or unfunctionalized CNTs. The slopes of the graphs gave rate constants values ranging between 0.5848 and 1.4452 (Table 2.10).

Table 2.6 Values of ln(1-Ut) for unfunctionalized nanotubes at various times.

S.No.	Time (Hrs.)	ln(1-Ut) for unfunctionalized nanotubes					
		Cr (VI)	As (III)	Ni (II)	Cd (II)	Pb (II)	Cu (II)
1	0.5	-0.6163	-0.6682	-0.9162	-0.4732	-0.3368	-0.3184
2	1.0	-0.9545	-1.3412	-1.4246	-0.8648	-0.6174	-0.6857
3	1.5	-1.0738	-1.6039	-1.7701	-1.2472	-1.4898	-1.0529
4	2.0	-1.8393	-2.0732	-2.5492	-1.6592	-1.7599	-1.2211
5	2.5	-1.9899	-2.5194	-2.9681	-2.0463	-2.2408	-1.7891
6	3.0	-2.3227	-2.9897	-3.4262	-2.2032	-2.7118	-2.1584

Table 2.7 Values of ln(1-Ut) for acylated nanotubes at various times.

S.No.	Time (Hrs.)	ln(1-Ut)for acylated nanotubes					
		Cr (VI)	As (III)	Ni (II)	Cd (II)	Pb (II)	Cu (II)
1	0.5	-0.7013	-0.7956	-1.2458	-0.4606	-0.4711	-0.4730
2	1.0	-1.1641	-1.2266	-1.6044	-0.9263	-0.7526	-0.9103
3	1.5	-1.4392	-1.6533	-2.1698	-1.0817	-1.2517	-1.0906
4	2.0	-1.7999	-2.0971	-2.7488	-1.4627	-1.9646	-1.4020
5	2.5	-2.3340	-2.4046	-3.3077	-1.7076	-2.4534	-1.7270
6	3.0	-2.5232	-2.7333	-3.4420	-2.0333	-2.9488	-2.0333

Table 2.8 Values of ln(1-Ut) for amide functionalized nanotubes at various times.

S.No.	Time (Hrs.)	ln(1-Ut)for amide functionalized nanotubes					
		Cr (VI)	**As (III)**	**Ni (II)**	**Cd (II)**	**Pb (II)**	**Cu (II)**
1	0.5	-0.6456	-1.0084	-1.08470	-0. 8416	-0.6967	-0.6667
2	1.0	-1.1106	-1.5100	-1.6231	-1.2086	-1.1244	-1.1270
3	1.5	-1.5056	-1.7081	-1.8035	-1.4898	-1.5521	-1.6225
4	2.0	-1.8663	-2.0005	-2.3501	-2.1100	-1.8766	-1.9264
5	2.5	-2.3456	-2.5016	-2.7719	-2.3166	-2.3361	-2.3433
6	3.0	-2.7709	-2.6327	-3.1937	-2.6526	-2.8352	-2.7662

Table 2.9 Values of ln(1-Ut) for azide functionalized nanotubes at various times.

S.No.	Time (Hrs.)	ln(1-Ut) for azide functionalized nanotubes					
		Cr (VI)	As (III)	Ni (II)	Cd (II)	Pb (II)	Cu (II)
1	0.5	-0.6193	-0.7003	-1.0881	-0.5504	-0.5411	-0.6881
2	1.0	-1.0183	-1.1539	-1.6665	-0.8792	-1.0546	-1.0936
3	1.5	-1.3712	-1.5945	-2.2968	-1.3415	-1.5654	-1.6104
4	2.0	-1.9533	-2.0433	-3.2586	-1.7401	-2.1663	-1.8553
5	2.5	-2.3549	-2.6118	-3.9812	-2.3891	-2.5823	-2.3618
6	3.0	-3.2467	-3.3039	-4.6834	-2.5158	-3.7422	-2.7211

Table 2.10 Comparative study of different MWNTs.

Rate Constant values(Slope of ln(1-Ut) v/s Time)				
Metal ions	**Unfunctionalized CNT**	**Oxidized CNT**	**Amide functionalized CNT**	**Azide functionalized CNT**
Cr^{+6}	0.6764	0.7214	0.9300	0.8032
As^{+3}	0.9406	0.8620	0.5848	0.8812
Ni^{+2}	1.0168	1.1580	0.8436	1.4452
Cd^{+2}	0.7832	0.6514	0.7340	0.7972
Pb^{+2}	0.9420	0.9776	0.8554	1.0216
Cu^{+2}	0.7386	0.6500	0.9206	0.8110

2.5.2.2 Effect of pH

Rejection experiments were also carried out at different pH. Different metal ion solutions of concentration 1ppm were prepared and their pH was adjusted by addition of 0.1N NaOH. Batch experiments were carried out at three pH -3.5, 7.2, 9.5 for Cr^{+6} and at pH -3.5, 7.2 for other metal ions, as other metal ions get precipitated out in form of hydroxides at basic pH. The observed results (Figure 2.13) confirmed that more adsorption was found at pH 3.5 (acidic), which could be explained as high complexation tendency of surface active sites of the nanotubes with the metal ions, under acidic conditions.

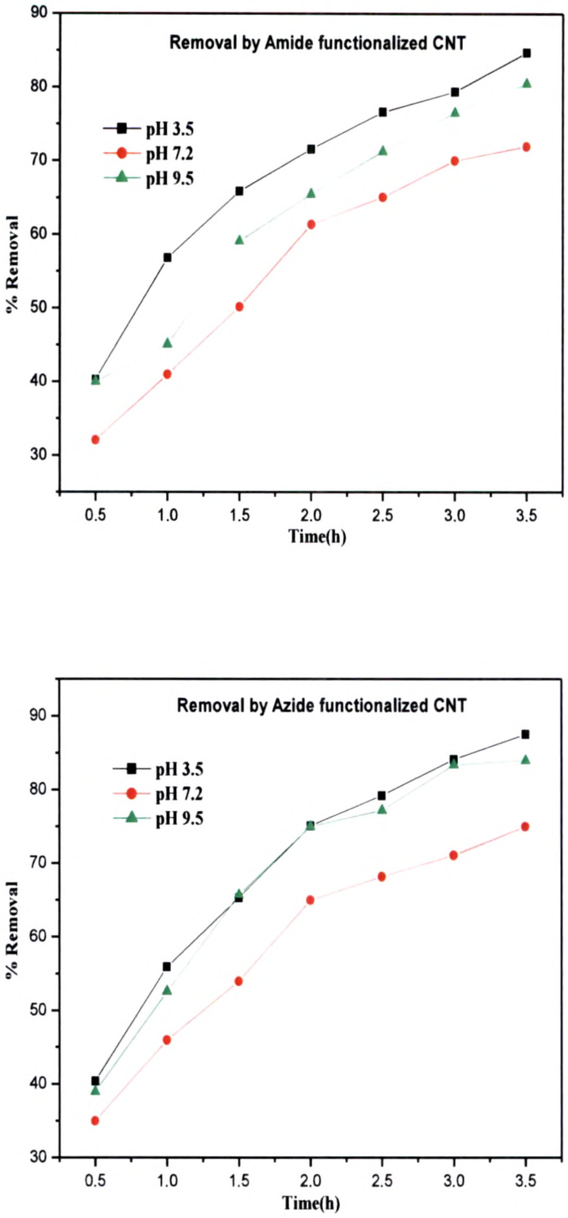

Figure 2.13 Removal of Cr^{+6} ions at diff. pH by (a)amide and (b) azide functionalized CNTs.

2.5.2.3 Effect of dosage

Role of adsorbent dose is also an important factor, which can affect the adsorption reaction. The studies were also directed towards determining the role of functionalized carbon nanotubes dose on metal removal from their aqueous solutions. Percent removal verses FCNTs is shown in Table 2.11. It can be easily observed that adsorption increases with increase in adsorbent dose up to a certain extent after which it is independent and no further increase in removal can be achieved. It was 10mg at which maximum adsorption was observed, and followed a plateau after that where no further increase was found on increasing the dosage.

Table 2.11 % Removal of metal ions with dosage of functionalized nanotubes.

S.No.	Dosage mg/10 ml	Removal capacity (%) of CNTs							
		Cr (VI)		Pb (II)		As (III)		Cd (II)	
		AmNT	AzNT	AmNT	AzNT	AmNT	AzNT	AmNT	AzNT
1.	1.0	60.7	62.3	58.1	59.8	24.2	25.3	22.7	24.6
2.	2.0	66.5	68.1	64.3	66.4	28.0	29.2	26.5	27.0
3.	2.5	71.5	72.3	66.7	68.5	30.2	31.9	27.0	28.3
4.	3.0	76.8	78.6	69.4	73.2	32.5	34.3	29.2	30.6
5.	5.0	80.6	83.7	76.8	81.0	35.7	38.2	31.8	35.4
6.	10.0	84.7	87.5	79.7	84.7	40.3	40.9	35.5	35.9
7.	12.0	84.8	87.5	79.7	84.7	40.4	40.9	35.5	35.9
8.	15.0	84.8	87.5	79.8	84.7	40.4	40.9	35.5	35.9
9.	20.0	84.9	87.5	79.8	84.7	40.4	41.0	35.5	35.9

* AmNT: Amide functionalized CNT's & AzNT: Azide functionalized CNT's

2.5.3 Adsorption isotherm studies with batch method

Batch adsorption isotherm experiments were conducted by using five concentrations (900, 1000, 1500, 1750 and 2500 µg/L) at pH 3.5. After treatment of a series of 10 mL of chromium solutions of different concentrations with 10 mg of the amide and azide functionalized CNTs, separately for 3.5h(time of reaching equilibrium), the concentration of the filtrates were analyzed by AAS. The amount of metal ion adsorbed by functionalized CNTs per gram (Q_e mg/g)was calculated, for all sets of both functionalized CNTs according to the following equation:

$$Qe = (Ci - Ce) \times V/m$$

Where Ci and Ce are initial and equilibrium concentration (mg/L), respectively. V (L) and m (g) are volume of the sample solution and mass of the functionalized CNT's. The observed adsorption data were fitted in Langmuir[137,138] and Freundlich[139] models.

The amount of Cr^{+6} adsorbed onto amide and azide functionalized CNTs(Table 2.12,2.13) from aqueous solutions show that the adsorption capacity of Cr^{+6} onto per gram functionalized carbon nanotubes increases with increasing the initialCr^{+6} concentration, and continues up to 2500 µg/L and level off thereafter, in both cases. Langmuir and Freundlich models are employed to describe the adsorption process. These isotherm relate metal uptake per unit weight of adsorbent Q*e* to the equilibrium adsorbate concentration in the bulk fluid phase Ce. The Langmuir model represents one of the first theoretical treatments of non-linear sorption. The Langmuir isotherm is given by :

$Qe= Q^o bCe/1+bCe$ (1)

Where Q^o and b are Langmuir constants related to maximum adsorption capacity and energy of adsorption respectively. Eq. 1 is generally linearised by inversion to get the following form:

$1/Qe= 1/Q^o+1/bQ^o * 1/Ce$ (2)

Table 2.12 Showing Xe, Qe, Ce, 1/Xe, 1/Qe, 1/Ce, Log Qe, Log Ce for different initial concentrations of Cr^{+6} solution when their adsorption was studied onto amide CNTs, to study Langmuir and Freundlich isotherms.

Initial conc. (µg)	**% Removal at equili. by amide CNT**	**Cr mg/L**	**Ce mg/L**	**Qe mg/g**	**1/Qe g/mg**	**1/Ce L/mg**	**Log Qe**	**Log Ce**
900	86.11	0.775	0.125	0.775	1.290	8	-0.110	-.0.903
1000	84.7	0.847	0.153	0.847	1.180	6.535	-0.072	-0.815
1150	80	0.920	0.230	0.920	1.086	4.347	-0.036	-0.638
1750	64.3	1.126	0.624	1.126	0.888	1.602	0.051	-0.204
2500	51.6	1.29	1.210	1.29	0.775	0.826	0.110	0.082

Table 2.13 Showing Xe, Qe, Ce, 1/Xe, 1/Qe, 1/Ce, Log Qe, Log Ce for different initial concentrations of Cr^{+6} solution when their adsorption was studied onto azide CNTs, to study Langmuir and Freundlich isotherms.

Initial conc. (μg)	**% Removal at equili. by azide CNT**	**Cr mg/L**	**Ce mg/L**	**Qe mg/g**	**1/Qe g/mg**	**1/Ce L/mg**	**Log Qe**	**Log Ce**
900	87.6	0.789	0.111	0.789	1.267	9.003	-0.102	-0.954
1000	87.5	0.875	0.125	0.875	1.142	8	-0.058	-0.903
1150	83.1	0.956	0.196	0.956	1.046	5.123	-0.01	-0.707
1750	68.5	1.200	0.550	1.200	0.83	1.783	0.08	-0.259
2500	56.8	1.421	1.079	1.421	0.703	0.926	0.1525	0.033

Equation 2 is generally used to analyze batch equilibrium data by plotting 1/Qe versus 1/Ce, which yields a linear plot if the data conform to the Langmuir isotherm. The linear plot of 1/Qe versus 1/Ce gives the intercept and slope corresponding to $1/Q^o$ and $1/(Q^o b)$ respectively, from which both Q^o and b are derived.

The Freundlich isotherm is the most widely used non linear sorption model and is given by the general form:

$\log Qe = \log K_F + 1/n \log Ce$ (3)

Where K_F relates to sorption capacity and 1/n to sorption intensity. The above logarithmic form is generally used to fit data from batch equilibrium studies. A plot of logQe vs logCe should yield a straight line if the Freundlich equation is obeyed by the adsorption equilibrium. The plot of logQe against log Ce gives the intercept and slope corresponding to log K_F and 1/n, respectively, from which both K_F and n are obtained. Values of 1/Qe, 1/Ce, Log Qe, Log Ce were calculated using reports from AAS analysis as in Table 2.12,2.13. Graphs were plotted between 1/Qe and 1/Ce, and Log Qe and Log Ce to get Langmuir and Freundlich isotherms (Figure 2.14,Figure 2.15).

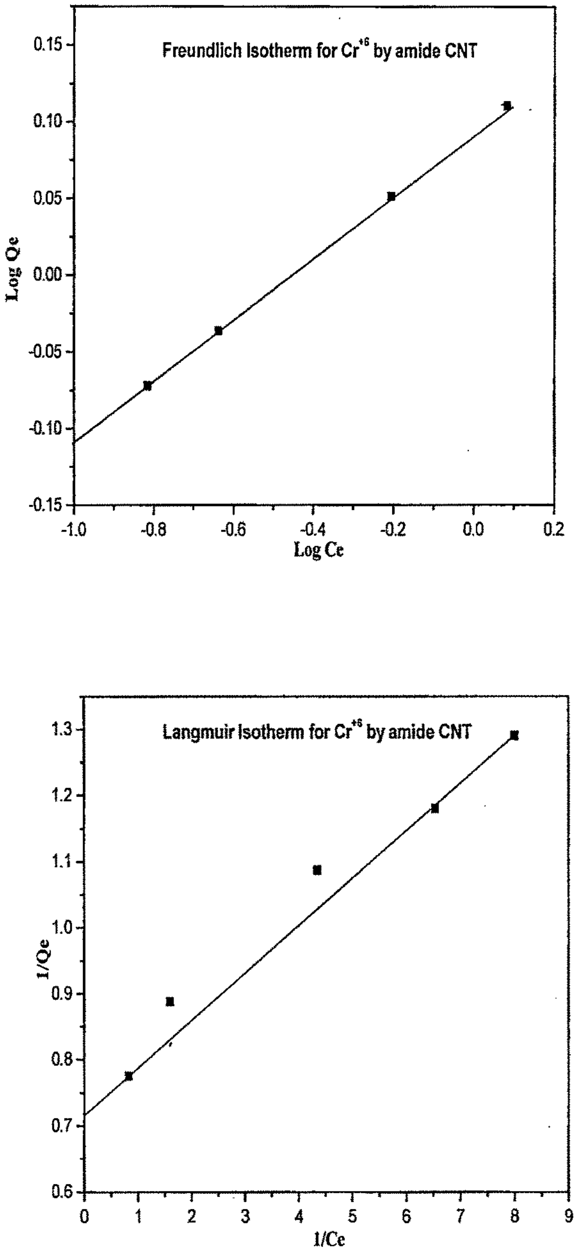

Figure 2.14 Freundlich and Langmuir adsorption isotherm of Chromium onto amide functionalized CNTs.

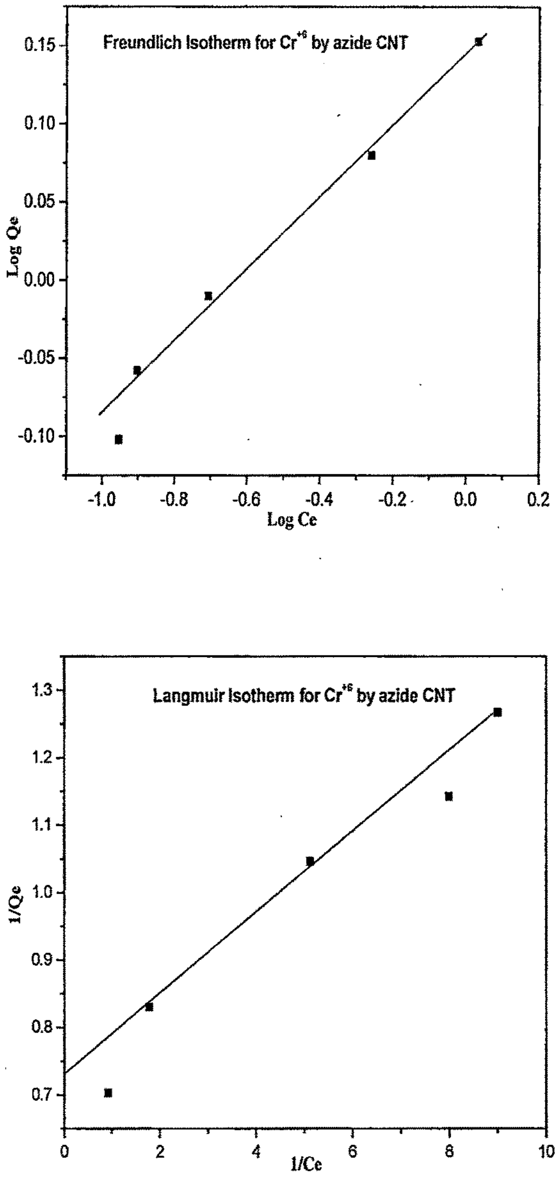

Figure 2.15 Freundlich and Langmuir adsorption isotherm of Chromium onto azide functionalized CNTs.

The parameters Q^o, K, R^2 and 1/n as calculated (Table 2.14) from Figure 2.14 & Figure 2.15 suggest that the Freundlich model is more suitable to fit the adsorption data than Langmuir model since the correlation coefficients (R^2) are higher 0.9878, 0.9967 for adsorption of heavy metal ions onto functionalized CNTs. The value Q^o gives maximum adsorption capacity of the carbon nanotubes, which comes out to be 1.386 mg/g. The numerical value of 1/n <1 indicates that adsorption of metal ions onto functionalized CNTs is multilayer adsorption process.

Table 2.14 The regression equations parameters Q^o, K, R^2 and 1/n for functionalized CNTs.

	Langmuir Model			**Freundlich Model**		
	Q^o(mg/g)	b(L/mg)	R^2	K_F	1/n	R^2
Amide CNT	1.386	9.63	0.9389	0.762	0.2024	0.9967
Azide CNT	1.386	11.933	0.9301	0.754	0.2436	0.9878

2.6 Conclusion

% Removal is a function of time and continuously increases with time of contact, upto a point where equilibrium is reached. At equilibrium the adsorption process becomes steady and does not increase with increase in contact period.

Maximum adsorption and thus percentage removal is observed for Chromium followed by that of Lead. In all the cases equilibrium is reached at 3.5h.The ln (1-U_t) is plotted against time t, for different metal ions, and straight line was obtained. This suggested that adsorption process followed first order kinetics. The slope of the plot gives overall rate constant. The removal capacity of azide and amide functionalized CNT is found to be greater than unfunctionalized, oxidized or acylated CNTs due to greater chelation capacity.

The adsorption isotherms of metal ions adsorbed onto functionalized CNTs from aqueous solution show that their adsorption onto per gram functionalized carbon nanotubes increases with increasing the initial Cr^{+6} concentration and continued up to 2500 μg/L and level off thereafter. Better rejection is found at acidic pH due to greater complexation tendency.

The regression equations parameters Q^o, K and 1/n and the correlation coefficient were calculated. It is seen that the Freundlich model is more suitable to fit the adsorption data than Langmuir model since the correlation coefficients are higher than 0.9800. The numerical value of $1/n < 1$ indicates that adsorption of metal ions onto functionalized CNTs is best fitted by Freundlich model and multilayer adsorption occurs on the surface following first order kinetics.